PHYSICAL REVIEW B **68**, 241406(R) (2003)

Diameter dependent wall deformations during the compression of a carbon nanotube bundle

U. D. Venkateswaran,[1] D. L. Masica,[1] G. U. Sumanasekera,[2] C. A. Furtado,[3] U. J. Kim,[3] and P. C. Eklund[3]
[1]*Department of Physics, Oakland University, Rochester, Michigan 48309, USA*
[2]*Department of Physics, University of Louisville, Louisville, Kentucky 40292, USA*
[3]*Department of Physics, Pennsylvania State University, University Park, Pennsylvania 16802, USA*
(Received 17 October 2003; published 31 December 2003)

Raman scattering is used to study the pressure-dependence of the radial (R) bands of *bundled* single-walled carbon nanotubes (SWNT) produced by the HiPCO process. We find that the normalized pressure derivative of the R-band frequency, $\Phi = d(\ln \omega_R)/dP$, increases with increasing nanotube diameter D as $\Phi \sim D^2$. Using results from elastic theory, we show that the contribution to Φ from isolated SWNT, $(=\Phi_0)$, is small, which agrees with previous model calculations. We show here that Φ_0 is independent of D. We conclude that most of the pressure dependence observed for the R bands in SWNT bundles may be identified with tube wall deformations mediated *via* tube-tube interactions within a bundle and not with the compression of an individual tube.

DOI: 10.1103/PhysRevB.68.241406 PACS number(s): 61.46.+w, 63.22.+m, 78.30.Na, 78.67.Ch

Carbon nanotubes are currently under intense study, driven in part by applications, such as field emission and nanoelectronic devices,[1] and in part by numerous unresolved fundamental issues regarding quantum confinement, ballistic transport, etc.[2] The study of the phonons in carbon nanotubes using Raman scattering techniques has been extensive in probing their electronic and vibrational properties.[3] Because of the intense, resonant Raman scattering from the radial (R) and tangential (T) vibrational modes of the carbon atoms, one is able to investigate the effects of externally applied pressure on these phonons. Single-walled carbon nanotubes (SWNTs) are produced in the form of bundles containing tens to hundreds of 1–10-μm-long tubes bound in a triangular lattice by the weak van der Waals force. Under hydrostatic pressure both the bundle *and* the individual nanotubes are compressed. The effects of this bundle compression have been studied previously in a diamond anvil cell up to pressures of ~20 GPa using Raman spectroscopy.[4] However, understanding the behavior of an isolated SWNT in a hydrostatic pressure environment requires the loading of single (isolated) tubes into the hole (~200-μm diameter) in the gasket of the diamond cell and is technically much more demanding than experiments made to date.

In this Rapid Communication, we report new experimental results on HiPCO-derived,[5] bundled SWNTs that demonstrate for the first time a clear nanotube diameter (D) dependence of the normalized (or logarithmic) pressure derivative Φ of the R-band frequency ω_R, i.e., $\Phi = (1/\omega_R)(d\omega_R/dP) = d(\ln \omega_R)/dP$. This behavior is tentatively assigned to pressure-driven deformations of the nanotube walls caused by tube-tube interactions in the bundle. Based on our data, we propose that this pressure-driven deformation decreases strongly with decreasing tube diameter (D). This study is possible because of the wide tube diameter distribution (~0.7–1.4 nm) present in HiPCO SWNTs. We also address the isolated tube behavior theoretically using a recently reported analytical expression[6] for the radial breathing mode (RBM) frequency (ω_R) of isolated SWNTs expressed in terms of the elastic properties of a graphene sheet rolled into a seamless nanotube.

Previous high pressure Raman experiments[4,7] have shown that the pressure derivative of the R-band frequency in SWNT bundles lies in the range of 7–10 cm^{-1}/GPa; the pressure derivative of the T-band frequency is somewhat smaller and is between 5 and 7 cm^{-1}/GPa. Noting this difference, Thomsen *et al.*[8] have argued that the pressure dependence of the radial vibrations in SWNT bundles should contain both intramolecular (isolated tube) as well as intermolecular [tube-tube van der Waals (vdW) coupling] contributions. Assuming that the total force constant is the sum of the intra- and intermolecular force constants, and using the pressure dependence of particular phonon modes measured in graphite,[9] they have estimated that the vdW component contributes ~37% to the force constant of the RBM. Other theoretical work[10] for bundled SWNTs at *ambient* pressure has shown that the RBM frequency should be related to the sum of a diameter-dependent contribution and a smaller constant term, i.e., $\omega_R \sim 234(\text{nm cm}^{-1})/D\ (\text{nm}) + \omega_0$, where $\omega_0 \sim 12-14\ \text{cm}^{-1}$. The value 234 cm^{-1} represents an average over several investigations, as reported in Ref. 11; the constant ω_0 approximates the effects of the tube-tube vdW interactions within a bundle. The pressure dependence of the vibrational modes of isolated and bundled SWNTs has been examined using molecular dynamics[12] and total energy[13] calculations. Both these calculations predict a small $d\omega_R/dP \sim 1\ \text{cm}^{-1}$/GPa for isolated SWNTs and an upshift (under ambient conditions) in ω_R of ~14 cm^{-1} (Ref. 12) and ~6 cm^{-1},[13] respectively, due to bundling. Kahn and Lu[13] studied SWNTs in the diameter range of 0.7–1.7 nm and their calculations, which did not include wall deformations, yield no significant diameter dependence for $d\omega_R/dP$.

HiPCO material, used in this work, was obtained from Rice University[5] and subjected to a three-step (sequential) purification process: (1) Controlled oxidation in flowing dry air at 400 °C for 30 min. (2) 10-h reflux in 2N HCl; washing in deionized water. (3) Heat treatment in flowing Ar at 1000 °C for 8 h (~10 sccm at ~1 atm). The purified material exhibited sharp R and T bands in the Raman spectrum in good agreement with previously published results.[14] A small flake (~75–100-μm linear dimension) of this purified mate-

rial and ruby chips were loaded into a gasketted Merrill-Bassett-type diamond anvil cell using methanol-ethanol as the pressure-transmitting medium.[15] Raman scattering experiments were carried out at 300 K using a conventional grating spectrometer and liquid nitrogen cooled CCD detector.

Typical Stokes Raman spectra in the low frequency R-band region for HiPCO SWNTs, revealing a rich structure associated with the wide tube diameter distribution, are presented for different pressures in Fig. 1(a). (The high frequency T bands also were found to exhibit a strong pressure dependence, but they are not discussed in this paper.) We calculate the diameter of the nanotube from the observed frequency of the R band in the 1-bar spectrum, using the expression discussed in Ref. 11 (see above). Knowing the diameter D, one can identify the metallic or semiconducting nature of the tube probed with a given laser excitation from the calculated E_{ii} versus D graph,[16] commonly called as the ''Kataura plot.'' This procedure was previously discussed with reference to the ambient pressure Raman data of HiPCO SWNTs.[14] Using the same procedure, we have identified the tubes probed using the green and red laser excitation and labeled them as metallic (m) and semiconducting (s) in the 1-bar spectra shown in Fig. 1(a). As the applied pressure is increased, the R bands shift to higher frequency, broaden, and weaken. It can be seen that the R bands due to large diameter tubes (low ω_R) broaden and weaken at a lower pressure than those due to small diameter tubes. For example, in the high pressure spectra shown in the top panel of Fig. 1(a), peaks 1 and 2 (due to large D tubes) have broadened and merged into a single shoulder at 3.5 GPa and both peaks are hardly discernable at 6.6 GPa, whereas peak 5 (due to smaller D tubes), which was weaker than 1 and 2 at 1 bar, can be seen to have almost the same relative intensity with respect to peak 4 at high pressure as it had at 1 bar. Similarly, a large broadening of the R bands due to larger D tubes compared to those from smaller D tubes, is seen in the spectra shown in the bottom panel of Fig. 1(a) as well. The pressure dependence of ω_R for selected R bands [peaks 1 and 4 in the top panel and the two strong peaks in the bottom panel of Fig. 1(a)], is shown in Fig. 1(b). Note the different vertical scales in each panel of Fig. 1(b).

In Fig. 2, we plot the normalized pressure derivative of ω_R, i.e., $\Phi = d(\ln \omega_R)/dP$, against ω_R. We choose to use Φ, rather than $d\omega/dP$, since Φ is related to the mode Grüneisen constant $\gamma [= B\ d(\ln \omega/dP) = B\Phi$, where B is the bulk modulus], which can be connected to the anharmonicities in the force constants. The different symbols in Fig. 2 refer to the values of Φ determined from several experiments. Solid symbols refer to previous measurements on SWNT bundles. Solid square, circle, and up-triangle in Fig. 2 correspond, respectively, to our published data.[7,12,17] Results from other groups on SWNT bundles prepared from pulsed laser vaporization[18] and arc discharge[19,20] methods are denoted by solid pentagon, down-triangle, and diamond, respectively. All these previously published data are from tubes in the narrow diameter range of ~1.3 to 1.5 nm. The results from this study on HiPCO-SWNT bundles using green (514.5-nm) (Ref. 21) and red (632.8-nm) laser excitations are shown as

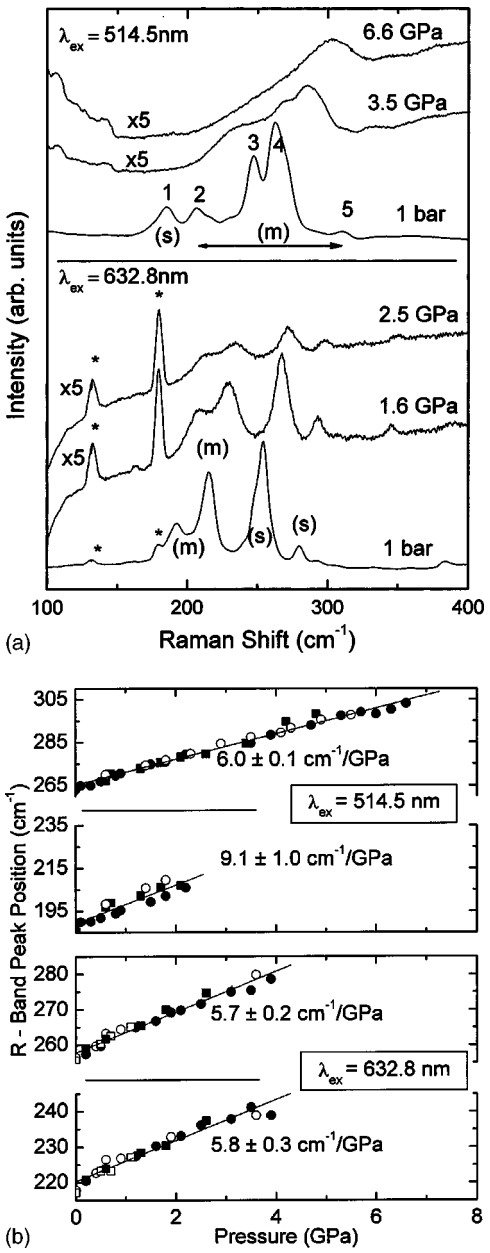

FIG. 1. (a) R-band spectra from HiPCO-SWNT bundles at various pressures using 514.5- and 632.8-nm laser excitations. (s) and (m) refer to R bands of semiconducting and metallic tubes. The spectral resolution is ~7 cm^{-1}. Peaks marked with ''*'' in the spectra excited with 632.8-nm laser designate neon plasma lines. (b) Pressure-induced shift in the peak frequency of selected radial bands. Solid and open symbols refer to data measured during compression and decompression. Circles and squares refer to measurements on different pieces of the sample, i.e., a check for reproducibility.

open circles in Fig. 2. The dashed curve through the experimental data is the result of a power law fit to the data, which is discussed later. The horizontal solid line at the bottom of the figure represents the result from our calculation for Φ (isolated SWNT) that is presented below.

Using the theory of elasticity, Mahan[6] showed that the radial breathing mode (RBM) frequency in an isolated SWNT can be approximated by

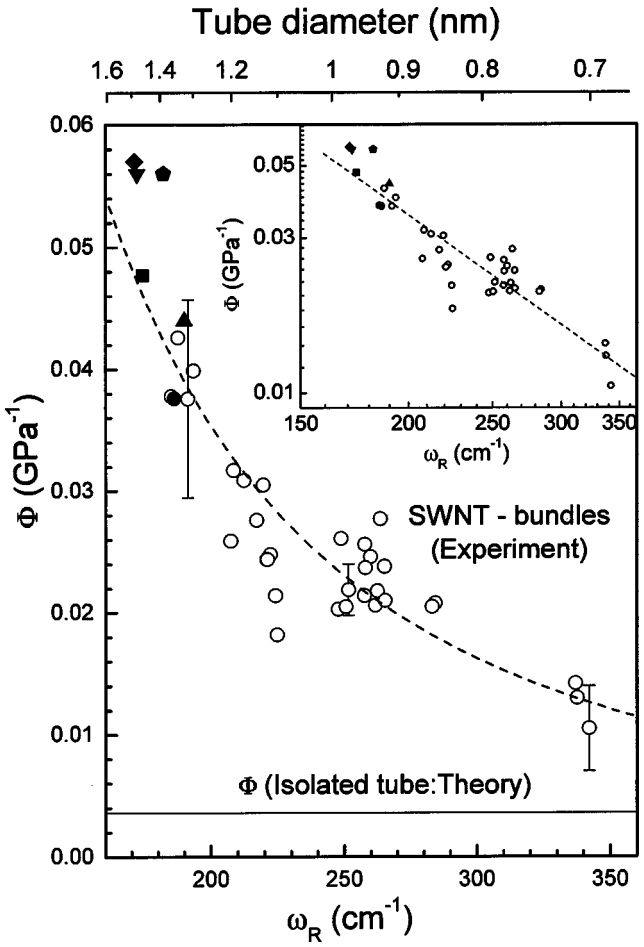

FIG. 2. Comparison of the experimental values for the normalized pressure derivative of the R-band frequency (Φ) in SWNT bundles and our theoretical prediction (Φ_0) for an isolated tube vs tube diameter (upper scale) or ambient R-band frequency, ω_R (lower scale). See the text for the explanation of the various symbols and lines. Large, medium, and small error bars on HiPCO data (open circles) refer to typical uncertainties in Φ for weak, moderate, and strong R bands. The inset is a log-log plot of Φ vs ω_R; the dashed lines in the figure correspond to least squares fit to the data with a slope of -1.9 ± 0.1.

$$\omega_R(\mathrm{cm}^{-1}) = (1/\pi c D)[(C_{11}^2 - C_{12}^2)/\rho C_{11}]^{1/2}, \qquad (1)$$

where D is the diameter of the SWNT; ρ and C_{11} and C_{12} are, respectively, the mass density and elastic constants of graphite. Because we express ω_R in cm^{-1}, a factor of c^{-1} (c= speed of light) appears in Eq. (1). To make contact with experimental data, Mahan[6] used the values of C_{ij}'s and ρ of graphite (instead of graphene) and obtained $\omega_R = 227\ (\mathrm{nm\ cm}^{-1})/D(\mathrm{nm})$, in good agreement with previous calculations and empirical treatments that relate RBM frequency and tube diameter.

As Eq. (1) contains four pressure-dependent quantities D, C_{11}, C_{12}, and ρ, the pressure derivative of ω_R will contain their pressure derivatives. We note that the diameter, D, of SWNTs can be expressed in terms of chiral indices (n,m) and the nearest neighbor carbon-carbon distance $a_{C\text{-}C}$, or equivalently the in-plane lattice constant in graphite a_0 ($=\sqrt{3}a_{C\text{-}C}$). Taking the pressure derivative of Eq. (1), we find

$$\frac{d\omega_R}{dP} = \frac{1}{D}[A_1(dC_{11}/dP) + A_2(dC_{12}/dP) + A_3(d(\ln a_0)/dP) + A_4(d(\ln \rho)/dP)], \qquad (2)$$

where $A_1 = (1/2\pi c\rho C)(1+C_r^2)$, $A_2 = -(1/\pi c\rho C)C_r$, $A_3 = -(1/\pi c)C$, $A_4 = (1/2)A_3$, $C = [(C_{11}^2 - C_{12}^2)/\rho C_{11}]^{1/2}$, and $C_r = (C_{12}/C_{11})$.

TABLE I. Parameters of graphite used for the numerical evaluation of Eq. (2).

C_{11} (GPa)	dC_{11}/dP	C_{12} (GPa)	dC_{12}/dP	$d(\ln a_0)/dP$ (GPa^{-1})	$d(\ln V)/dP$ (GPa^{-1})
1060[a] (±20)	39[b] (±10–15%)	180[a] (±20)	11[b] (±10–15%)	0.0008[c] (±6%)	0.0296[c] (±1%)

[a]Reference 21. [b]Reference 22. [c]Reference 9.

Inserting the values of the various quantities occurring in Eq. (2) from Refs. 9, 22, and 23 (see Table I), we find, $(d\omega_R/dP) = [1/D][4.41 - 0.411 + 0.181 - 3.39]$ (cm^{-1}/GPa), where D is to be expressed in nm. The first term on the right hand side is due to C_{11} and is the largest positive contribution to $d\omega_R/dP$; the second term, due to C_{12}, is about a tenth of the first term and is negative; the third term, *i.e.*, the contribution from a_0 (or D) is a small positive quantity; and the last term corresponds to the effects of the volume compressibility of graphite and produces a contribution that is comparable to the first term, but with opposite sign. The net result from the insertion of the experimental values in Eq. (2) is

$$d\omega_R/dP = [1/D][0.83(\mathrm{cm}^{-1}/\mathrm{GPa})]. \qquad (3)$$

Thus for an isolated SWNT, the logarithmic pressure derivative of ω_R is given by, $\Phi_0 = (1/\omega_R)(d\omega_R/dP) = 0.0036\ (\mathrm{GPa})^{-1}$, where we have used Eq. (3) and substituted $\omega_R = 234\ (\mathrm{nm\ cm}^{-1})/D(\mathrm{nm})$. Therefore, Φ_0 is a constant independent of the tube diameter (and hence ω_R). Since Eq. (2) is derived using elastic theory of graphene cylinder, it is important to remember that this expression ignores any changes in the elastic constants of an isolated nanotube that stem from wall curvature. Secondly, the development of Eq. (2) from Eq. (1) should be accurate when anharmonic effects are small. Since graphite exhibits one of the largest lattice thermal conductivities of any solid,[24] we can assume that anharmonic effects should be small until strong curvature effects are encountered (curvature introduces an admixture of sp^3 character into the system).

The horizontal solid line in Fig. 2 denotes the value of $\Phi_0 = 0.0036\ (\mathrm{GPa})^{-1}$, obtained above for an isolated SWNT. The diameter scale at the top of this figure is estimated using $\omega_R = 234\ (\mathrm{cm}^{-1}\text{-nm})/D(\mathrm{nm}) + 12\ \mathrm{cm}^{-1}$. The various experimental data points span a factor of ~2 in

SWNT diameter range (~0.7 to 1.5 nm). Furthermore, we notice that a *bundled* tube with $D=1.4$ nm has a value of $\Phi\sim 12$ times larger than Φ_0 (isolated tube), whereas a smaller diameter *bundled* tube with $D\sim 0.7$ nm has a value of Φ only a factor of 3 larger than Φ_0. The comparison of the dashed and solid lines in Fig. 2 suggests that tube-tube interactions in a bundle dominate the normalized pressure derivative of ω_R. A simple explanation for this behavior is that the circular cross section of larger diameter tubes are easier to deform under compression. One can imagine that the six nearest neighbor tubes surrounding a central tube in the rope lattice produce six facets on the central tube at the ''contact'' points. Consistent with the data in Fig. 2, and the reported polygonization of SWNT bundles,[12,25] this faceting is much easier to accomplish with larger diameter tubes.

The inset to Fig. 2 shows Φ versus ω_R in a log-log plot. The straight line is a least squares fit to the data; the resulting exponent is $-1.9\pm 0.1\approx 2$, i.e., $\Phi\sim D^2$. One might expect any simple theory for Φ based on the elastic properties of an sp^2 carbon cylinder to eventually fail at small D. We observe from our data that Φ for small diameter tubes is approaching the value of Φ_0, (see Fig. 2), it therefore appears a simple sp^2 theory might be able to explain the tube deformations in a bundle under pressure for tubes as small as a (5,5) tube, i.e., curvature effects are not very significant.

In summary, using bundled SWNTs prepared by the HiPCO process we have been able to investigate the pressure dependence (up to ~7 GPa) of the radial breathing mode frequency, ω_R, over a reasonably wide range (0.7–1.4 nm) of tube diameter D. We find that the normalized (or logarithmic) pressure derivative of ω_R exhibits a strong D^2 dependence. Using an analytical expression for ω_R obtained from a simple elastic model, we find that the normalized pressure derivative of ω_R *for an isolated tube* is independent of the tube diameter, whereas experiments on bundled tubes show a strong D^2 dependence for this quantity. We are therefore led to the conclusion that the tube-tube interactions within a bundle and pressure-induced tube wall deformations are responsible for the observed behavior. We further infer from our data that the tube wall deformation is particularly dominant in large diameter tubes when subjected to external pressure.

The work at Oakland University was supported by NSF-DMR-014706 and by the Donors of the Petroleum Research Fund, administered by the American Chemical Society. The work at the Pennsylvania State University was supported by NSF-NIRT Grant No. DMR-0103585. We are grateful to R. E. Smalley and his group at Rice University for the HiPCO sample. We thank G. D. Mahan and V. Crespi for helpful discussions.

[1] *Carbon Nanotubes*, Topics in Applied Physics, Vol. 80, edited by M. S. Dresselhaus, G. Dresselhaus, and P. Avouris (Springer-Verlag, Berlin, 2001).
[2] J. Hone, B. Batlogg, Z. Benes, A. T. Johnson, and J. E. Fischer, Science **289**, 1730 (2000).
[3] M. S. Dresselhaus and P. C. Eklund, Adv. Phys. **49**, 705 (2000).
[4] I. Loa, J. Raman Spectrosc. **34**, 611 (2003), and references therein.
[5] P. Nikolaev, M. J. Bronikowski, R. K. Bradley, F. Rohmund, D. T. Colbert, K. A. Smith, and R. E. Smalley, Chem. Phys. Lett. **313**, 91 (1999).
[6] G. D. Mahan, Phys. Rev. B **65**, 235402 (2002).
[7] U. D. Venkateswaran, E. A. Brandsen, U. Schlecht, A. M. Rao, E. Richter, I. Loa, K. Syassen, and P. C. Eklund, Phys. Status Solidi B **223**, 225 (2001).
[8] C. Thomsen, S. Reich, A. R. Goñi, H. Jantoljak, P. M. Rafailov, I. Loa, K. Syassen, C. Journet, and P. Bernier, Phys. Status Solidi B **215**, 435 (1999).
[9] M. Hanfland, H. Beister, and K. Syassen, Phys. Rev. B **39**, 12598 (1989).
[10] L. Henrard, E. Hernandez, P. Bernier, and A. Rubio, Phys. Rev. B **60**, R8521 (1999); H. Kuzmany, W. Plank, M. Hulman, Ch. Kramberger, A. Grüneis, Th. Pichler, H. Peterlik, H. Kataura, and Y. Achiba, Eur. Phys. J. B **22**, 307 (2001).
[11] S. Bandow, G. Chen, G. U. Sumanasekara, R. Gupta, M. Yudasaka, S. Iijima, and P. C. Eklund, Phys. Rev. B **66**, 075416 (2002).
[12] U. D. Venkateswaran, A. M. Rao, E. Richter, M. Menon, A. Rinzler, R. E. Smalley, and P. C. Eklund, Phys. Rev. B **59**, 10928 (1999).
[13] D. Kahn and P. Lu, Phys. Rev. B **60**, 6535 (1999).
[14] G. Chen, G. U. Sumanasekara, B. K. Pradhan, R. Gupta, P. C. Eklund, M. J. Bronikowski, and R. E. Smalley, J. Nanosci. Nanotechnol. **2**, 621 (2002).
[15] See, A. Jayaraman, Rev. Mod. Phys. **55**, 65 (1983).
[16] H. Kataura, Y. Kumazawa, Y. Maniwa, I. Umezu, S. Suzuki, Y. Ohtsuka, and Y. Achiba, Synth. Met. **103**, 2555 (1999).
[17] U. Schlecht, U. D. Venkateswaran, E. Richter, J. Chen, R. C. Haddon, P. C. Eklund, and A. M. Rao, J. Nanosci. Nanotechnol. **3**, 139 (2003).
[18] M. J. Peters, L. E. McNeil, J. P. Lu, and D. Kahn, Phys. Rev. B **61**, 5939 (2000).
[19] A. K. Sood, P. V. Teradesai, D. V. S. Muthu, R. Sen, A. Govindaraj, and C. N. R. Rao, Phys. Status Solidi B **215**, 393 (1999).
[20] C. Thomsen, S. Reich, H. Jantoljak, I. Loa, K. Syassen, M. Burghard, G. S. Duesberg, and S. Roth, Appl. Phys. A: Mater. Sci. Process. **69**, 309 (1999).
[21] A preliminary report was presented in U. D. Venkateswaran, M.-É. Gosselin, B. Postek, D. Masica, G. Chen, R. Gupta, and P. C. Eklund, Phys. Status Solidi B **235**, 364 (2003).
[22] O. L. Blakslee, D. G. Proctor, E. J. Seldin, G. B. Spence, and T. Weng, J. Appl. Phys. **41**, 3373 (1970).
[23] W. B. Gauster and I. J. Fritz, J. Appl. Phys. **45**, 3309 (1974).
[24] M. S. Dresselhaus and G. Dresselhaus, Adv. Phys. **30**, 139 (1981).
[25] J. Tang, L.-C. Qin, T. Sasaki, M. Yudasaka, A. Matsushita, and S. Iijima, Phys. Rev. Lett. **85**, 1887 (2000).